Energy and angular distributions of electrons from ion impact on atomic and molecular hydrogen. II. 20–114-keV $H^+ + H$

G. W. Kerby III, M. W. Gealy,* Y.-Y. Hsu, and M. E. Rudd

Department of Physics and Astronomy, University of Nebraska, Lincoln, Nebraska 68588-0111

D. R. Schultz and C. O. Reinhold

Physics Division, Oak Ridge National Laboratory, Oak Ridge, Tennessee 37831-6373

Results of crossed-beam measurements of cross sections differential in ejected electron energy and angle for ionization of atomic hydrogen by 20–114-keV protons are reported. Secondary electrons were measured over an energy range of 1.5–300 eV and an angular range of 15°–165°. Atomic-hydrogen targets were produced in a radio-frequency discharge source with a dissociation fraction of about 74%. Ratios of cross sections for H targets to those for H_2 targets were obtained from measurements on the mixed target. From these ratios, the measured dissociation fractions, and the absolute cross sections measured for H_2 targets, the cross sections for H targets were determined. These measurements are compared with the results of the first-order Born approximation, the continuum-distorted-wave eikonal-initial-state approximation, and the classical trajectory Monte Carlo (CTMC) methods. Good overall agreement is found with the CTMC results, except for slow, backward electron emission. The addition of the classically suppressed dipole transitions from the Born approximation to the CTMC results yields a good estimate of the ejected electron spectrum.

PACS number(s): 34.50.Fa

I. INTRODUCTION

The simplest ionization process is the ejection of an electron from a hydrogen atom in a collision with a proton. Unlike electron-impact collisions, there is no exchange interaction of target and projectile particles to complicate the picture and the projectile transfers only a small fraction of its momentum and energy during the collision. Furthermore, the proton carries no electrons to add to the complexity of the interaction. In spite of its simplicity, the reaction $H^+ + H \rightarrow H^+ + H^+ + e^-$ is still a three-body system in its final state and therefore does not admit an analytical solution. To solve the dynamical problem involved, one must use approximations.

In the early history of theoretical attempts to describe the ionization process, the only measurements available were of the total-ionization cross sections (TICSs). Since these involve an integration over the momenta of all three particles in the final state, many of the details of the interaction were hidden. In the 1960s measurements of the angular and energy distributions of the ejected electrons from such collisions began to become available [1]. Since such doubly differential cross sections (DDCSs) contain much more information and provide a far more stringent test of theory, their availability has led to a fuller understanding of the mechanisms of ionization.

TICSs for protons on atomic hydrogen have been measured by Fite *et al.* [2], Shah, Elliott, and Gilbody, [3], and by Shah and Gilbody [4]. Park *et al.* [5] made energy-loss measurements from which information was extracted on the energy (but not angular) distributions of

ejected electrons. Although DDCSs for proton impact have been measured for a wide range of target gases and incident energies (see the review in Ref. [1]), atomic-hydrogen targets have not previously been investigated experimentally in this detailed way. Shyn [6] used a microwave discharge hydrogen-atom source to make DDCS measurements for 25–250-eV electron impact. We report here a similar series of measurements for proton impact on atomic hydrogen using a commercially available [7] rf hydrogen-atom source developed by Slevin and Stirling [8].

Preliminary data at 70 keV, reported earlier [9], are superseded by the present data which are somewhat more accurate at the lower electron energies and are given for additional incident energies. We also reported observations of a large, broad peak in the electron energy spectrum centered at about 31 eV in the backward direction with respect to the incident beam [10]. While this feature is still not completely understood, its rapid disappearance with increasing source pressure suggests that it arises from an excited component of the target beam which is collisionally quenched at higher target densities. The data in the present work have been obtained at sufficiently high pressures that this feature is not present.

This is paper II of a series of four. In paper I [11] the apparatus and method for all of the measurements were discussed and the data for $H^+ + H_2$ were presented. In papers III and IV data for $He^+ + H_2$ and $He^+ + H$ are planned to be given.

II. THEORY

Measurements of the ejected electron spectrum in collisions of protons with atomic hydrogen at intermediate

---

*Present address: Concordia College, Moorhead, MN 56562.

velocities provide a very fundamental testing ground for theoretical descriptions. Here we seek to make a detailed comparison with the three most widely applied theoretical methods for intermediate-energy collisions: the first-order Born approximation (B1), the continuum-distorted-wave–eikonal-initial-state (CDW-EIS) approximation [12,13], and the classical trajectory Monte Carlo (CTMC) method [14,15]. These models have been described and applied in great detail elsewhere; we focus here on discussing their ranges of validity.

For very high impact velocities v_p, or when the projectile charge Z_p is small enough, the B1 approximation is well suited to describe most of the features of the ejected electron spectrum in ion-atom collisions. Provided that the projectile charge is of the order of the target nuclear charge, a single criterion may be used to specify this regime of validity, namely, $\eta = Z_p/v_p \ll 1$, where η is commonly referred to as the Sommerfeld parameter. The essence of the B1 approximation is the treatment of the projectile ion–electron interaction as a small perturbation. At intermediate collision velocities ($v_p \sim v_e$, where v_e is the initial orbital electron velocity) this approximation is not valid because the electron wave function is strongly distorted by the passing ion. A large body of work, both experimental and theoretical, has shown that in order to describe the angle and energy distributions of electrons ejected in intermediate energy ion-atom collisions, the electrons must be treated as being emitted in the combined field of both the target and projectile ions (see, e.g., [13] and [16] and other references therein).

To treat this regime in which such "two-center" effects are important (or dominant), higher-order perturbation approaches have been developed, such as the CDW-EIS and the strong-potential Born approximations. In the CDW-EIS approximation, the interaction of the electron with both the projectile and residual target ions are treated on an equal footing in the final state through a product of Coulomb continuum states of both centers. Consequently, a range of validity which extends to velocities lower than that of the B1 approximation is expected, i.e., down to $\eta \sim 1$ [13].

Another common approach, the CTMC method, consists of treating the interactions of the electron with both the projectile and target ions exactly, though classically. This method utilizes an ensemble of initial electronic orbits which approximates the quantum-mechanical position and momentum distributions as closely as possible. The motions of the projectile, target electron, and target core are then followed by solving the classical equations of motion for a sequence of time steps through the collision. Once the particles have separated, knowledge of their positions and momenta allows determination of the DDCS for ionization. In contrast to the perturbation methods, this approach is most applicable when the projectile ion-electron interaction is strong. When this occurs, a very large number of quantum states become populated and their superposition may be successfully mimicked quasi-classically [17]. For weak perturbations, this approach breaks down, as will become clear through the comparisons with experiment and the other theories presented here.

In a sense, quasiclassical and quantum-mechanical perturbation methods complement one another, and the best that one may presently achieve is to make a combined model which exploits the best features of each approach. In particular, a number of authors (see, e.g., [17–19]) have identified a deficiency of the CTMC model which is the classical suppression of dipole-allowed transitions. A well-known consequence of this fact is the difference between the quantum-mechanical $E^{-1}\ln E$ and classical E^{-1} dependences of the TICS at high impact energies. At intermediate impact velocities this translates into a sizable classical underestimation of the cross sections for emission of electrons into very large, backward, angles. To overcome these classical deficiencies, we present here results of a combined model in which the quantum-mechanical (B1) results for small momentum transfers are added to the CTMC cross sections [17], which we denote CTMC+B1. In this model, we compute the Born approximation limited to momentum transfers Δp, smaller than a critical value given by

$$\Delta p_c = \left[\frac{Z_t^2}{2n^2} - \frac{Z_t^2}{2(n+1)^2} \right]^{1/2} ,$$

where Z_t is the target nuclear charge and n is the initial electronic principal quantum number, as described in Ref. [17]. In this case, since $Z_t = 1$ and $n = 1$, $\Delta p_c = \sqrt{3/8}$. The result of this Born calculation is then added to the CTMC result, in a sense correcting it since below this momentum transfer the classical ionization probability begins to drop significantly below the quantum-mechanical result. In terms of ejected electron energies, this critical momentum transfer corresponds to a final electron energy of 1.3 eV for 20-keV proton impact and 22 eV for 114-keV proton impact, for example.

Clearly all of the present approaches break down in the limit of low collision velocities, $v_p \ll v_e$. In this regime, the evolution of the systems takes place through transitions governed by molecular dynamics. The appropriate description of such dynamics is the close-coupling approach in which the Schrödinger equation is solved by expanding the wave function in a finite basis set. Unfortunately, it is extremely difficult to achieve a good representation of the continuum, and calculations which yield accurate DDCSs are presently impractical.

III. RESULTS

The apparatus, experimental method, theory of the measurement, and the reliability were discussed in paper I [11] and will not be repeated here. Absolute values of the DDCSs are given for five incident energies in the range 20–114 keV in Tables I–V. The DDCSs were also numerically integrated over angle or electron energy to obtain the singly differential cross sections (SDCSs) and over both angle and energy to obtain the TICSs. These are also given in the tables.

The TICSs are compared with the direct measurements of Shah and Gilbody [4] and with our B1, CDW-EIS, CTMC, and CTMC+B1 calculations in Table VI. The present experimental data agree reasonably well with the

TABLE I. Measured values of $\sigma(W,\theta)$ in units of 10^{-20} cm^2/eV sr, $\sigma(W)$ in units of 10^{-20} cm^2/eV, $\sigma(\theta)$ in units of 10^{-20} cm^2/sr, and σ_I (lower right-hand corner) in units of 10^{-20} cm^2 for secondary-electron production in 20-keV H$^+$ +H collisions. Numbers in brackets are powers of 10 by which quantities are to be multiplied.

W (eV)	15°	20°	30°	50°	70°	90°	110°	130°	160°	$\sigma(W)$
1.5	797	596	286	72.9	30.9	15.5	8.88	8.50	13.9	924
2	813	529	247	64.5	25.7	13.5	8.30	6.96	9.30	873
3	756	455	200	53.2	21.3	11.9	7.83	6.25	6.84	770
5	595	314	133	40.3	16.2	8.67	5.12	5.29	4.74	586
7.5	296	175	94.6	30.4	11.9	7.18	3.87	3.92	3.56	356
10	179	122	72.2	23.2	8.07	5.97	2.94	2.83	2.54	243
15	92.9	70.7	43.7	12.3	4.39	2.39	1.61	1.35	1.06	129
20	56.3	42.3	25.3	6.41	2.31	1.38	0.930	0.829	0.523	74.4
30	18.1	13.3	7.89	1.76	0.663	0.409	0.231	0.254	0.115	22.8
50	1.28	1.00	0.545	0.118	0.0419	0.0422	0.0104			1.75
75	0.0673	0.0324	0.0197	6.55[−3]						0.067
100	0.0226	0.0123		7.74(−4)						0.0123
$\sigma(\theta)$	6700	4510	2270	629	248	141	80.4	79.8	87.4	7810

measurements of Shah and Gilbody, differing by no more than 29% at most. At the lower energies, the B1 approximation greatly overestimates the total cross section, but for impact energies above about 67 keV, it agrees well with experiment. CTMC agrees well with experiment for incident energies above 20 keV, but is too small for lower energies, owing to the suppression of low-energy backward electrons as described above. While very good agreement is found between CDW-EIS and the experimental TICS data throughout the range of impact energies surveyed here, we will show that CDW-EIS does not reproduce the measured SDCSs and DDCSs well and therefore the agreement with the TICSs must be considered to be fortuitous.

In Fig. 1 we illustrate the behavior of the SDCS for three impact energies covering the extremes of the present measurements. For the highest energy displayed, 114 keV, $v_p/v_e = 2.14$, the projectile velocity is high enough so that the range of validity of the B1 approximation has been reached at its lower limit, while the CTMC and CDW-EIS approximations are well within their expected validity limits. Especially good agreement is observed among all the theoretical descriptions and with the experimental measurements of the energy distribution of the ejected electrons. This spectrum shows that the emission of electrons is dominated by ejection of low-energy electrons. A shoulder or plateau is observed at around 200 eV which is due to the binary encounter peak in the DDCS, summed over all angles of ejection. Beyond this region the cross section drops off rapidly in accordance with the initial target momentum distribution. The agreement between theories and experiment for 114 keV is not as complete for the angular distribution of electrons and a well-known failure of the B1 approxima-

TABLE II. Same as Table I, but for 48 keV.

W (eV)	15°	20°	30°	50°	70°	90°	110°	130°	150°	165°	$\sigma(W)$
1.5	583	631	439	172	71.7	32.1	17.7	13.8	15.2	15.3	1270
2	583	608	402	159	63.3	26.7	14.8	11.8	12.5	12.1	1170
3	549	568	369	130	50.7	20.3	11.0	8.85	9.13	9.86	1010
5	482	469	279	98.5	37.7	13.1	6.79	5.54	5.73	5.65	784
7.5	409	387	211	73.6	25.7	8.16	4.10	3.44	3.48	3.33	596
10	360	309	166	59.3	20.0	5.23	2.78	2.14	2.20	2.24	489
15	248	200	106	39.7	11.0	2.53	1.41	1.03	1.03	0.914	319
20	150	125	74.3	27.0	6.30	1.41	0.793	0.587	0.549	0.409	207
30	58.1	58.0	38.5	13.4	2.30	0.534	0.315	0.203	0.153	0.121	92.6
50	18.6	19.1	13.4	3.04	0.423	0.121	0.0722	0.0391	0.0207		27.5
75	6.18	6.13	3.41	0.416	0.0682	0.0252	0.0168	4.72[−3]	5.74[−3]		6.81
100	1.59	1.36	0.576	0.632	0.0130	5.72[−3]	2.73[−3]	2.13[−3]	1.14[−3]		1.40
130	0.203	0.137	0.0582	6.70[−3]	2.29[−3]						0.174
160	0.0202	0.0134	5.52[−3]	6.40[−4]					1.66[−4]		0.0162
200			4.46[−4]								
$\sigma(\theta)$	9040	8580	5260	1840	605	211	114	88.2	92.4	92.1	14 400

TABLE III. Same as Table I, but for 67 keV.

W (eV)	20°	30°	50°	70°	90°	110°	130°	150°	165°	σ(W)
1.5	560	380	181	79.0	37.3	21.4	16.1	17.5	16.3	1340
2	526	361	166	70.5	33.0	18.6	13.1	14.9	13.8	1230
3	468	312	142	58.8	25.4	13.6	10.1	10.9	10.6	1050
5	388	251	109	42.7	17.3	8.46	6.06	6.41	6.07	817
7.5	305	193	82.8	31.8	11.2	5.08	3.77	3.73	3.63	619
10	255	154	67.2	24.8	7.73	3.14	2.36	2.45	2.34	498
15	181	103	47.3	15.2	3.73	1.44	1.10	1.04	0.999	337
20	131	71.7	34.3	9.62	2.03	0.842	0.584	0.529	0.411	237
30	68.2	40.6	19.3	4.07	0.695	0.297	0.194	0.153	0.0818	124
50	22.6	17.0	6.94	0.769	0.150	0.0664	0.0380	0.0186		42.8
75	9.73	6.99	1.67	0.127	0.0384	0.0164	6.87[−3]	5.82[−3]		15.3
100	4.90	2.73	0.364	0.0330	0.0108	4.78[−3]	2.43[−3]	1.25[−3]		6.25
130	1.53	0.595	0.0554	6.58[−3]	2.77[−3]	1.24[−3]	5.97[−4]	7.31[−4]		1.69
160	0.313	0.0994	9.28[−3]			3.89[−4]	2.42[−4]			0.326
200	0.0284	0.0102	2.70[−3]			5.04[−5]				0.0338
250	1.15[−3]									
300	6.85[−5]		1.36[−3]							2.60[−3]
σ(θ)	8130	5120	2260	751	267	134	100	103	95.9	16 300

tion is seen at small angles. In this portion of the spectrum, it is critical to represent the outgoing electron as evolving in the combined field of both the projectile and residual target ions since production of "saddle-point" and "cusp" electrons play a very important role. The CDW-EIS and CTMC approximations account for these interactions and give better agreement with experiment. At backward angles, the CDW-EIS approximation is in very good agreement with the measurements while the underestimation of this portion of the spectrum by the CTMC approximation is clearly visible. By adding to the CTMC approximation that portion of the B1 approxima-

tion associated with small momentum transfers, this underestimation is remedied and the CTMC+B1 approximation gives reasonable overall agreement with the measurements.

Also depicted are the results for an impact velocity which is considerably lower, that is, for 20-keV impact energy, where $v_p/v_e = 0.895$ represents a lower boundary for the expected ranges of validity for the CTMC and CDW-EIS approximations. Therefore it is perhaps surprising that the CTMC model reproduces the energy distribution of electrons reasonably well, whereas the B1 and CDW-EIS approximations seem to underestimate the

TABLE IV. Same as Table I, but for 95 keV.

W (eV)	15°	20°	30°	50°	70°	90°	110°	130°	150°	165°	σ(W)
1.5	517	409	347	188	60.6	49.4	29.1	20.7	21.7	21.2	1280
2	449	350	303	174	72.0	40.4	23.8	17.9	18.2	19.8	1170
3	330	283	241	147	68.9	30.1	16.6	12.5	12.8	13.2	932
5	256	224	182	105	51.7	19.6	10.1	7.51	7.31	7.44	675
7.5	205	179	138	80.0	38.0	13.0	5.94	4.48	4.54	4.41	503
10	167	145	111	65.5	29.8	9.02	3.97	2.90	2.74	2.90	399
15	119	102	75.4	46.0	20.3	4.65	1.89	1.42	1.35	1.43	270
20	94.4	75.7	54.3	34.0	13.7	2.73	0.999	0.815	0.769	0.835	196
30	61.7	46.4	32.2	20.5	6.93	1.00	0.404	0.341	0.342	0.393	116
50	23.7	18.8	14.0	9.51	1.87	0.227	0.117	0.0997	0.105	0.141	46.6
75	8.87	8.49	7.28	4.05	0.416	0.0595	0.0364	0.0336	0.0398	0.0531	19.4
100	5.15	5.07	4.65	1.47	0.114	0.0233	0.0154	0.0134	0.0143	0.0226	9.83
130	3.43	3.26	2.53	0.382	0.0301	8.85[−3]	5.84[−3]	5.38[−3]	5.54[−3]	6.99[−3]	4.77
160	2.22	1.81	1.02	0.0935	0.0105	3.61[−3]	-2.16[−3]	1.66[−3]	2.28[−3]	2.87[−3]	2.20
200	0.654	0.559	0.216	0.0177	2.25[−3]	1.09[−3]	6.51[−4]		6.81[−4]	1.16[−3]	0.528
250	0.0915	0.747	0.0253	2.83[−3]		3.93[−4]				6.14[−4]	0.0701
300	0.0110	8.94[−3]	3.07[−3]	5.38[−4]							8.68[−3]
σ(θ)	6590	5490	4270	2430	871	339	176	128	131	130	14 800

TABLE V. Same as Table I, but for 114 keV.

W (eV)	15°	20°	30°	50°	70°	90°	110°	130°	150°	165°	σ(W)
1.5	244	242	194	120	70.8	37.9	28.6	20.8	19.8	20.1	859
2	245	241	193	119	69.9	37.6	24.3	17.1	16.3	16.0	834
3	226	225	174	111	64.3	31.9	18.3	13.5	12.3	13.2	744
5	178	170	138	86.9	48.7	21.3	10.2	7.95	7.41	7.94	559
7.5	132	130	105	67.5	36.6	14.4	6.16	4.57	4.25	4.11	413
10	112	107	83.4	55.1	29.9	10.6	3.69	2.88	2.82	2.73	329
15	79.4	70.3	56.8	39.0	20.1	5.60	1.81	1.28	1.19	1.10	222
20	55.7	52.9	40.2	28.2	13.8	3.22	0.909	0.708	0.613	0.509	153
30	37.6	31.7	23.2	17.4	8.08	1.17	0.322	0.225	0.191	0.163	91.1
50	17.0	13.7	9.98	8.51	2.47	0.211	0.0696	0.0458	0.0296	0.0229	38.6
75	6.65	5.85	5.23	4.20	0.547	0.0434	0.0177	0.0108	5.83[−3]		16.9
100	3.46	3.34	3.40	2.05	0.139	0.0133	4.70[−3]	2.95[−3]	1.55[−3]		8.90
130	2.27	2.39	2.36	0.674	0.0303	4.59[−3]	2.40[−3]	1.22[−3]			4.59
160	1.80	1.61	1.45	0.178	9.80[−3]	2.25[−3]	1.13[−3]	1.25[−3]			2.60
200	1.18	0.911	0.473	0.0305	2.70[−3]	1.02[−3]	5.91[−4]				1.06
250	0.306	0.218	0.0712	4.41[−3]	6.77[−4]						0.218
300	0.0478	0.0305	9.27[−3]	8.4[−4]							0.0333
400	9.97[−4]	6.02[−4]									4.62[−4]
σ(θ)	4150	3820	3010	1990	936	323	170	127	119	121	11 700
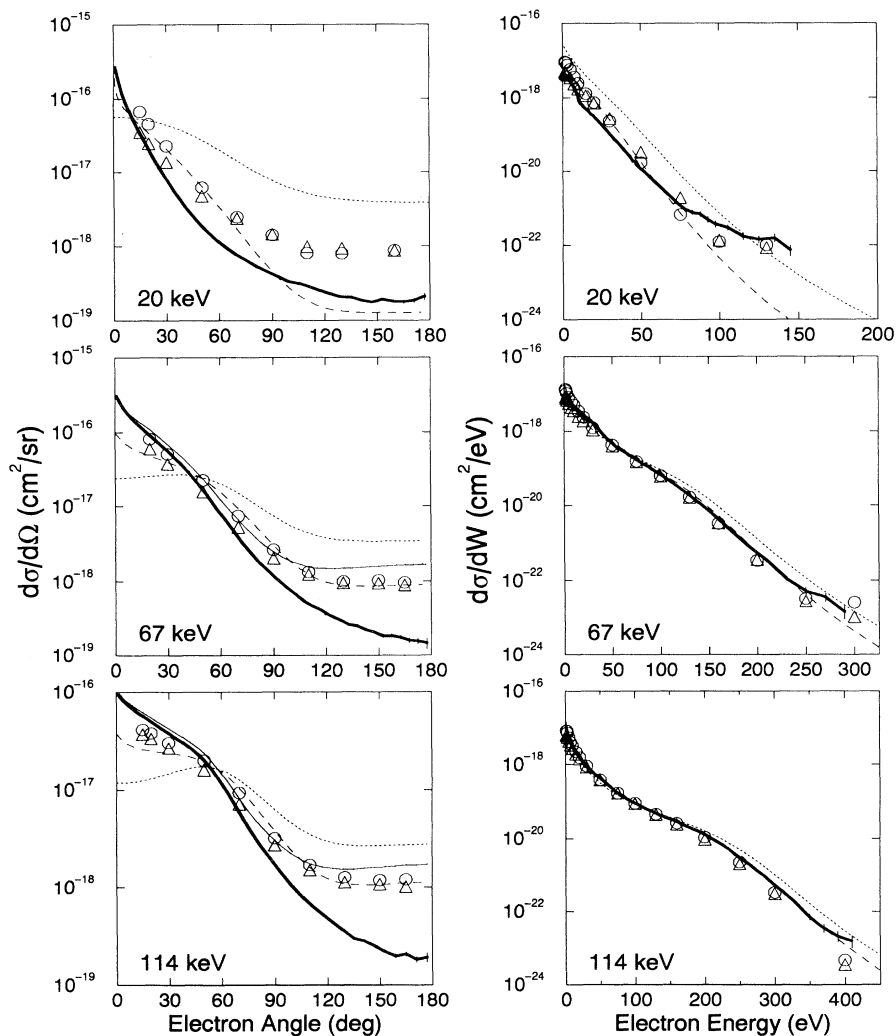
FIG. 1. Singly differential cross sections as a function of electron ejection angle and energy for 20-, 67-, and 114-keV proton impact on H and H_2. Circles, present experiment for H targets; triangles, present experiment [11] for H_2 targets divided by 2; heavy solid line, CTMC calculations; light solid line, CTMC+B1 calculations; dashed line, CDW-EIS calculations; dotted line, B1 approximation. All theoretical calculations are for atomic-hydrogen targets.

TABLE VI. The total cross section σ_i (in units of 10^{-16} cm^2) for ionization of atomic hydrogen by 20-, 48-, 670, 95-, and 114-keV protons. The present data are compared with the direct measurements of Shah and Gilbody [4], the recommended values given by Rudd et al. [22], and our present B1, CDW-EIS, and CTMC+B1 results.

Energy (keV)	Present	Ref. [4]	Ref. [22]	B1	CDW-EIS	CTMC	CTMC+B1
20	0.781	0.670	1.05	1.84	0.592	0.359	
48	1.44	1.40	1.36	1.72	1.40	1.37	1.59
67	1.63	1.34	1.30	1.47	1.36	1.53	1.84
95	1.48	1.15	1.15	1.19	1.17	1.34	1.62
114	1.17	1.06	1.06	1.08	1.05	1.16	1.43

yield of very hot electrons. Note that some of these hot electrons may originate in multiple binary collisions of the electron with both nuclei, a process which can occur in the CTMC method but is completely missing in the B1 and CDW-EIS approximations. Regarding the angular distribution, even though the CTMC and CDW-EIS approximations produce SDCSs which are reasonable in shape, evidently these models do not contain enough information on the collision dynamics at this low an impact energy. Clearly, the B1 approximation is even less satisfactory.

For an impact energy of 67 keV, a situation intermediate to the two extremes (20 and 114 keV) is obtained. Also note that we have included in Fig. 1 the present experimental measurements for H$_2$ targets, divided by 2. The departures of the H$_2$ data from the H data is thus a measure of how different H$_2$ is from two uncorrelated hydrogen atoms. Part of this difference is attributable to the difference in the ionization potentials, i.e., $I_{H_2}^2/I_H^2 = 1.29$. Effects due to the orientation of the molecule may also play a role.

Just as the SDCSs represent more stringent tests of theory than do the TICSs, the DDCSs likewise provide even more detailed discriminants. In Fig. 2 we display the DDCss for several small ejection angles (1°, 5°, 15°, 30°, and 50°) for 20, 67, and 114 keV. In the upper portion of the figure, the present experiment is compared to our CTMC results, whereas in the lower portion it is
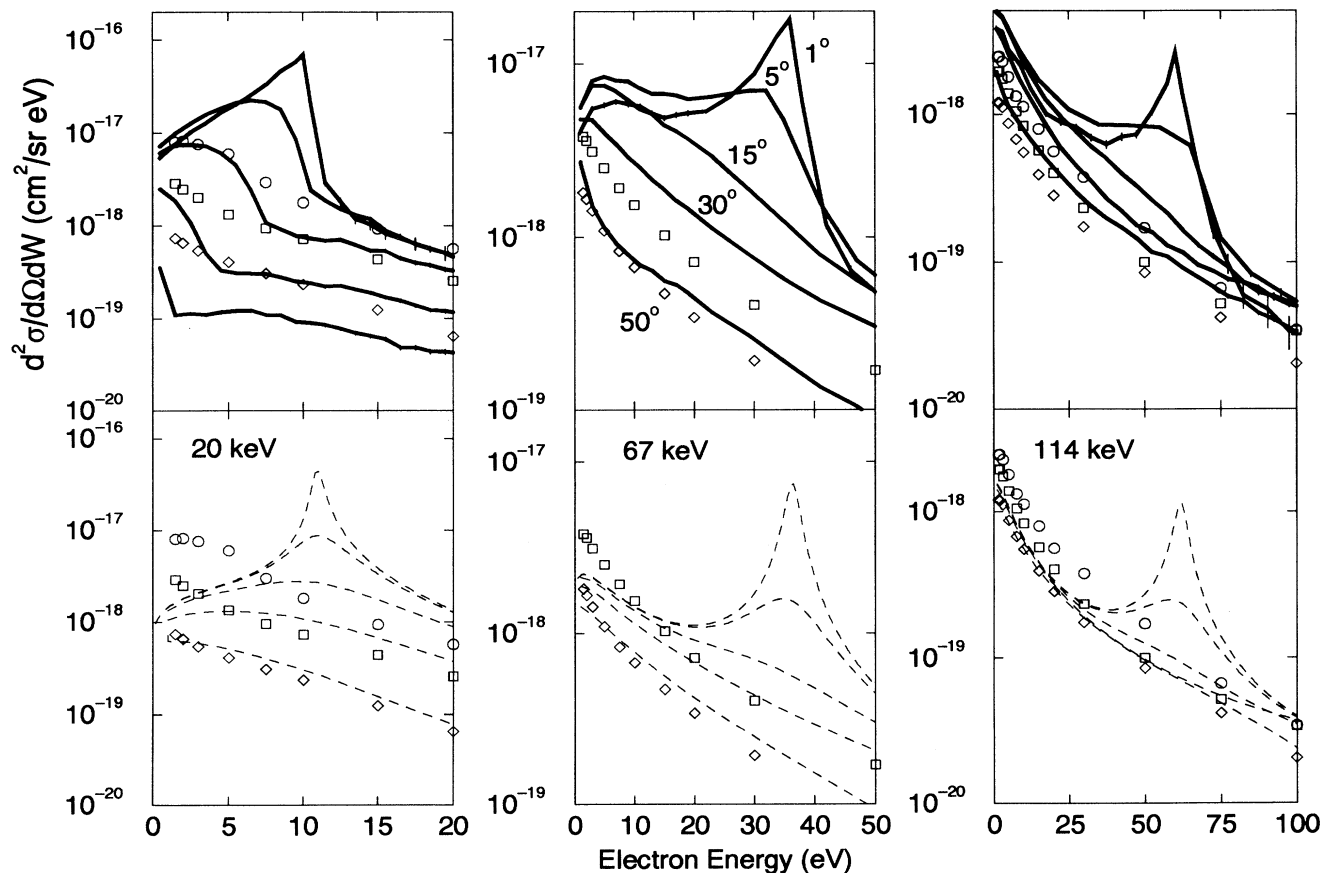

FIG. 2. Doubly differential cross sections as a function of electron ejection energy for 20-, 67-, and 114-keV proton impact on atomic hydrogen for several small ejection angles (1°, 5°, 15°, 30°, and 50°). The symbols are as indicated in Fig. 1.

compared with results of the CDW-EIS calculation. Clearly the most prominent feature of the forward ejected electron spectrum is the well-known electron-capture-to-the-continuum (ECC) cusp, which is observed for $v_e \sim v_p$. At the lowest impact energy, the spectrum is dominated near 0° by the ECC peak. For increasing impact energy, CTMC displays a shoulder at electron energies lower than the peak, and for the highest energy shown, the largest feature is the peak surrounding $v_e = 0$.

Especially for the lower impact energies the CTMC results indicate that as a function of increasing ejection angle, the peak in the spectrum moves to lower energies. In other words, the dominance of the ECC peak gives way first to the saddle-point peak, which in turn gives way to the soft electron peak. Since a number of groups have recently sought to measure a peak in the spectrum near the saddle-point region ($v_p/2$), it is important to emphasize that our CTMC calculations indicate that the existence of such a peak may be strongly dependent on the angle of ejection. In contrast, the CDW-EIS results show very little contribution to the spectrum at the lowest electron energies and yields a peak position which is much less sensitive to ejection angle. These effects have been observed previously and constitute shortcomings of the CDW-EIS model in representing the degree of asymmetry of the cusp (e.g., [20] and [21]). As illustrated by this figure, the agreement between theory and experiment is not good for 20 keV, but improves as the impact energy is increased.

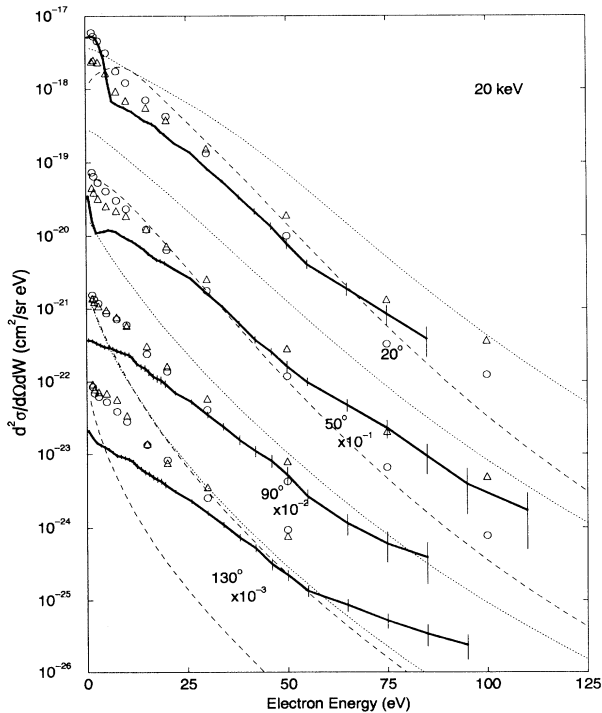In Figs. 3–7 we compare theories and experiment over

FIG. 3. Doubly differential cross sections as a function of electron ejection energy for 20-keV proton impact on H and H_2, at a wide range of ejection angles (20°, 50°, 90°, and 130°). The symbols are as indicated in Fig. 1.
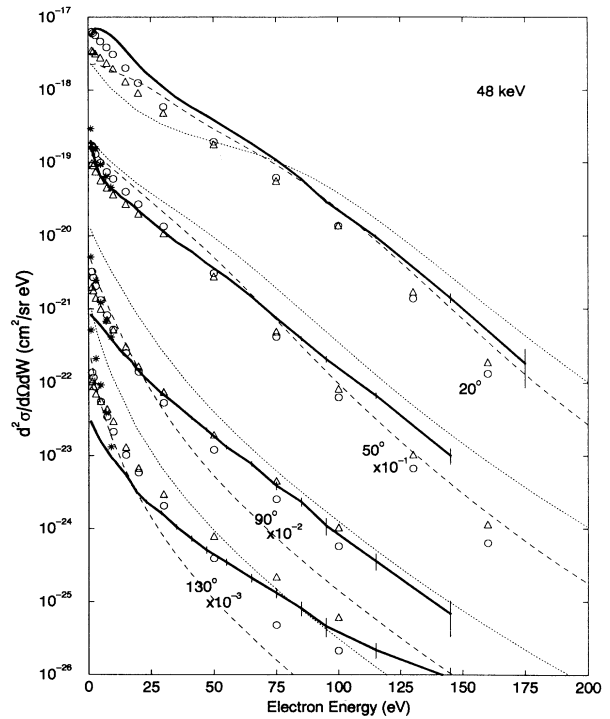

FIG. 4. Same as Fig. 3, except for 48-keV proton impact. The CTMC + B1 calculations are represented by asterisks.

a wider range of ejection angles (20°, 50°, 90°, and 130°). At the highest impact energy, there is rather good agreement among all the theories and with the experiment. As noted in the discussion of the SDCS, at small angles the
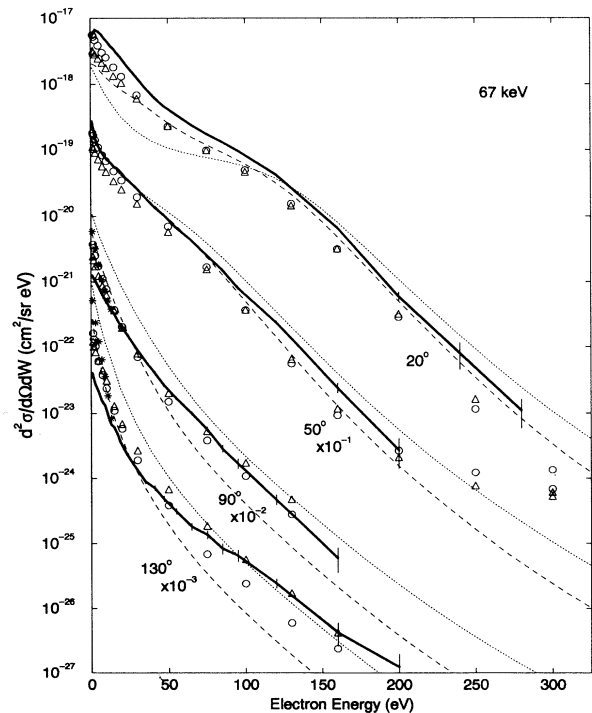

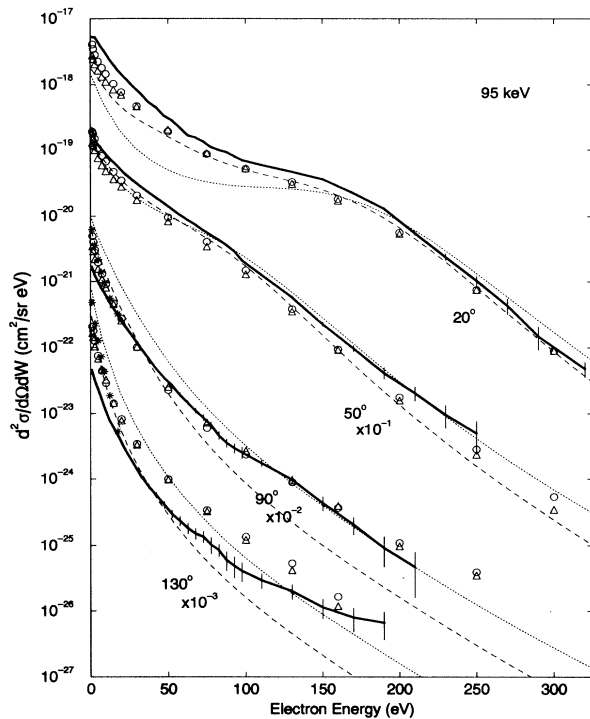FIG. 5. Same as Fig. 4, except for 67-keV proton impact.

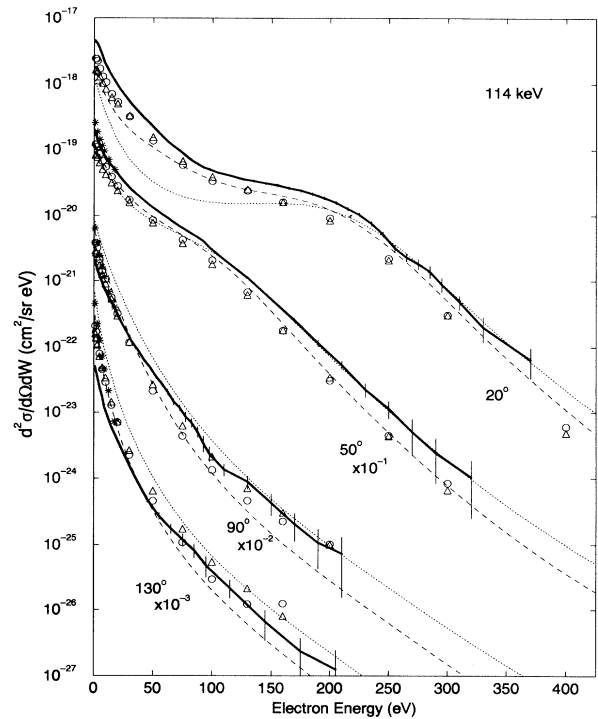FIG. 6. Same as Fig. 4, except for 95-keV proton impact.

FIG. 7. Same as Fig. 4, except for 114-keV proton impact.

B1 approximation yields too small a cross section. Here we see that this underestimation occurs primarily for small electron energies, i.e., those near the cusp and saddle-point regions. Also for small angles, but for larger electron energies, the B1 approximation seems to represent the binary-encounter shoulder reasonably well at an ejection energy of about 200 eV. For larger angles of emission, the B1 approximation yields much better agreement with experiment, indicating that the description of the electron as being ejected in the field of the target alone is a reasonable assumption. The CTMC and CDW-EIS results are in fairly good agreement with experiment throughout the angular range plotted. However, it is now evident that the deficiency noted regarding the underestimation of the large-angle cross section noted above in the discussion of the SDCS arose primarily for slow electron emission.

For lower impact energies the theoretical results begin to diverge to a larger extent from the experimental measurements and from each other. For example, at 20-keV, the perturbation theories are as much as two orders of magnitude different from one another at backward angles. In that case, the CDW-EIS approximation also predicts cross sections which are too small by a least an order of magnitude for electron energies greater than 10 eV.

IV. CONCLUSIONS

In this work we have presented measurements of cross sections, differential in the angle and energy of the ejected

electrons, for ionization of atomic hydrogen by incident protons. We have used the data to compare different theoretical approaches to the calculation of these cross sections in intermediate-energy collisions. Since the system studied is the simplest collision system involving the interaction of a single electron with two protons, it provides the most fundamental test possible. Since close-coupling treatments are still impractical, we have utilized the three most often applied approaches, the first-order Born, CDW-EIS, and CTMC approximations. Especially at the lowest impact energy, it is clear that fuller treatments of ionization must be developed, in particular concerning low-energy electron emission. For higher impact energies, the CDW-EIS and the CTMC+B1 approaches provide a reasonable description of the ejected electron spectrum, accounting in particular for the two-center effects.

Additional DDCS measurements on atomic hydrogen should be made at lower projectile energies to provide detailed data for testing future low-energy theoretical treatments. Higher-energy data, especially for electrons in the forward and backward directions, may show that some theoretical methods traditionally considered to be accurate at high energies are, in fact, not completely reliable at any energy. It would also be highly desirable to investigate the effect of the two-center interactions, especially on the angular distribution of electrons, by using higher-Z bare projectiles incident on atomic-hydrogen targets. Such work is now underway in a collaboration with C. L. Cocke, S. J. Hagmann, R. A. Moshammer, and P. Richard.

[1] M. E. Rudd, Y.-K. Kim, D. H. Madison, and T. J. Gay, Rev. Mod. Phys. **64**, 441 (1992).

[2] W. L. Fite, R. F. Stebbings, D. G. Hummer, and R. T. Brackmann, Phys. Rev. **119**, 663 (1960).

[3] M. B. Shah, D. S. Elliott, and H. B. Gilbody, J. Phys. B **20**, 2481 (1987).

[4] M. B. Shah and H. B. Gilbody, J. Phys. B **14**, 2361 (1981).

[5] J. T. Park, J. E. Aldag, J. M. George, J. L. Peacher, and J. H. McGuire, Phys. Rev. A **15**, 502 (1977); see also J. T. Park, Adv. At. Mol. Phys. **19**, 67 (1983).

[6] T. W. Shyn, Phys. Rev. A **45**, 2951 (1992).

[7] Leisk Engineering (currently VSW Technology, Ltd.), Albert Drive, Burgess Hill, West Sussex, RH15 9NX, England.

[8] J. Slevin and W. Stirling, Rev. Sci. Instrum. **52**, 1780 (1981).

[9] D. R. Schultz, R. E. Olson, C. O. Reinhold, M. W. Gealy, George W. Kerby III, Ying-Yuan Hsu, and M. E. Rudd, J. Phys. B **24**, L599 (1991).

[10] M. E. Rudd, M. W. Gealy, G. W. Kerby III, and Ying-Yuan Hsu, Phys. Rev. Lett. **68**, 1504 (1992).

[11] M. W. Gealy, G. W. Kerby III, Y.-Y. Hsu, and M. E. Rudd, preceding paper, Phys. Rev. A **51**, 2247 (1995).

[12] D. S. F. Crothers and J. F. McCann, J. Phys. B **16**, 3229 (1983).

[13] P. D. Fainstein, V. H. Ponce, and R. D. Rivarola, J. Phys. B **24**, 3091 (1991).

[14] R. Abrines and I. C. Percival, Proc. Phys. Soc. London **88**, 861 (1966).

[15] R. E. Olson and A. Salop, Phys. Rev. A **16**, 531 (1977).

[16] D. R. Schultz, C. O. Reinhold, and R. E. Olson, in *Two-Center Effects in Ion-Atom Collisions,* edited by Timothy Gay, Anthony Starace, and M. Eugene Rudd (American Institute of Physics, New York, in press).

[17] C. O. Reinhold and J. Burgdörfer, J. Phys. B **26**, 3101 (1993).

[18] L. G. J. Boesten and T. F. M. Bonsen, Physica B **79**, 292 (1975).

[19] L. G. J. Boesten, T. F. M. Bonsen, and D. Banks, J. Phys. B **8**, 628 (1975).

[20] D. R. Schultz and C. O. Reinhold, Phys. Rev. A **50**, 2390 (1994).

[21] C. O. Reinhold and R. E. Olson, Phys. Rev. A **39**, 3861 (1989).

[22] M. E. Rudd, Y.-K. Kim, D. H. Madison, and J. W. Gallagher, Rev. Mod. Phys. **57**, 965 (1985).